Open access • Journal Article • DOI:10.1126/SCIENCE.1167733

Observation of Unconventional Quantum Spin Textures in Topological Insulators

David Hsieh, Yuqi Xia, Lewis Wray, Lewis Wray ...+12 more authors

Institutions: Princeton University, Lawrence Berkeley National Laboratory, Paul Scherrer Institute, University of Zurich ...+2 more institutions

Published on: 13 Feb 2009 - Science (American Association for the Advancement of Science)

Topics: Topological order, Symmetry protected topological order, Topological degeneracy, Topological quantum number and Topological entropy in physics

Observation of unconventional quantum spin textures in topological insulators

Hsieh, D; Xia, Y; Wray, L; Qian, D; Pal, A; Dil, J H; Osterwalder, J; Meier, F; Bihlmayer, G; Kane, C L; Hor, Y S; Cava, R J; Hasan, M Z

Observation of unconventional quantum spin textures in topological insulators

Abstract

A topologically ordered material is characterized by a rare quantum organization of electrons that evades the conventional spontaneously broken symmetry-based classification of condensed matter. Exotic spin-transport phenomena, such as the dissipationless quantum spin Hall effect, have been speculated to originate from a topological order whose identification requires a spin-sensitive measurement, which does not exist to this date in any system. Using Mott polarimetry, we probed the spin degrees of freedom and demonstrated that topological quantum numbers are completely determined from spin texture-imaging measurements. Applying this method to Sb and Bi1-xSbx, we identified the origin of its topological order and unusual chiral properties. These results taken together constitute the first observation of surface electrons collectively carrying a topological quantum Berry's phase and definite spin chirality, which are the key electronic properties component for realizing topological quantum computing bits with intrinsic spin Hall-like topological phenomena.

Observation of unconventional quantum spin textures in topologically ordered materials

D. Hsieh,[1] Y. Xia,[1,2] L. Wray,[1,3] D. Qian,[1] A. Pal,[1] J.H. Dil,[4,5] F. Meier,[4,5] J. Osterwalder,[5] G. Bihlmayer,[6] C.L. Kane,[7] Y.S. Hor,[8] R.J. Cava,[8] and M.Z. Hasan[1,2]

[1]*Joseph Henry Laboratories of Physics, Department of Physics, Princeton University, Princeton, NJ 08544, USA*

[2]*Princeton Center for Complex Materials, PRISM, Princeton University, Princeton, NJ 08544, USA*

[3]*Lawrence Berkeley National Laboratory, Advanced Light Source, Berkeley, CA 94305, USA*

[4]*Swiss Light Source, Paul Scherrer Institute, CH-5232, Villigen, Switzerland*

[5]*Physik-Institut, Universität Zürich-Irchel, 8057 Zürich, Switzerland*

[6]*Institut für Festkörperforschung, Forschungszentrum Jülich, D-52425 Jülich, Germany*

[7]*Department of Physics and Astronomy, University of Pennsylvania, Philadelphia, PA 19104, USA*

[8]*Department of Chemistry, Princeton University, Princeton, NJ 08544, USA*

(Dated: July 12, 2008)

Abstract

Topological insulators are a fundamentally new quantum phase of matter that may provide a route to fault-tolerant quantum computing. A topologically ordered insulator or metal is uniquely identified by the spin structure of the Fermi contours that spontaneously exist on the sample boundaries. Here we report *spin texture* measurements on insulating and metallic $Bi_{1-x}Sb_x$ using Mott polarimetry and demonstrate a new method to probe topological quantum numbers not available from transport data. The spin textured edge Fermi contours reveal a new quantum order described by a mirror Chern topological number, and a surface Berry's phase of π that is found to survive through the bulk insulator to metal transition. In addition, our spin maps reveal the parity-class origin of topological order in this series and provide critical spin information needed for device engineering with topological materials.

The Bloch band insulator is arguably the most well understood electronic phase of matter [1, 2]. Recent theory predicts that there exists a rare type of band insulator, known as a Z_2 topological insulator, which can be fundamentally distinguished from an ordinary band insulator based on the topological properties of its electron wavefunction [3–6]. A textbook example of a topological property of a ground state wavefunction is the integer quantum Hall effect insulator [7]. In this case a magnetic field applied to a two-dimensional electron gas creates discrete energy levels called Landau levels. A topological quantum number (TQN) known as the Chern integer n, associated with an insulating state consisting of n filled Landau levels, represents the number of protected metallic chiral edge states that give rise to the quantized Hall conductance [7–10] $\sigma_{xy} = ne^2/h$, where e is the electric charge and h is Planck's constant. Until now, measuring σ_{xy} remains the conventional method of probing a TQN [7, 9, 10]. Unlike the integer quantum Hall phase, the bulk excitation gap in topological insulators is opened by spin-orbit coupling rather than an external magnetic field, and the TQNs (ν_i) that describe the bulk bands take on only two possible values [3–6, 11]. The two-dimensional version, known as the quantum spin Hall insulator, is commonly understood as two copies of the integer quantum Hall effect where the spin-orbit coupling acts as an internal magnetic field that points in a spin dependent direction, giving rise to counter propagating spin polarized edge states. Three-dimensional topological insulators on the other hand have no simple charge quantum Hall analogue, and are further complicated by the need for multiple TQNs (ν_i) to characterize their ground state [4, 6, 12]. Theoretical descriptions of their 2D edge (surface) states have only now begun to emerge.

The metallic boundary states of topological insulators have recently been proposed as a possible source of non-Abelian excitations that can be used to test schemes for fault-tolerant (topological) quantum computing [13], as a system for realizing spin-charge separation in two dimensions [14, 15], and have provided a theoretical framework for realizing exotic magnetic [16] and superconducting [17] states. These novel properties arise from the peculiar spin texture and geometry of the Fermi surface (FS) of the boundary metal, which is predicted to be spin polarized with states on opposite sides of the FS carrying opposite spin. For a 3D Z_2 topological insulator with mirror symmetry, this leads to a non-trivial spin texture for the 2D surface states, in which the spin direction is momentum dependent and rotates by 2π around the FS with a chirality that is related to a new TQN associated with the *spatial* symmetry. Unlike the Chern integers ($n = 1, 2, 3...$) found in charge quantum Hall

systems, the two-valued TQNs ($\nu_i = 0, 1$) characterizing the topological insulators are not associated with a quantized spin-Hall conductance or any other known quantized charge or spin transport response [3]. Therefore, directly mapping the spin textures of the boundary states is critical for determining the numerical values of the novel TQNs, and for measuring the quantitative degree of polarization important for assessing their potential use in device geometries that may be employed to test the aforementioned schemes.

Recent charge conductance [18] and charge-coupling photon-energy-modulated photoemission experiments [19] have provided preliminary evidence for metallic boundary states in candidate two- and three-dimensional topological insulators respectively. However their band spin properties have not been measured, and the bulk band origin of their topological order is unknown. Here we demonstrate a direct imaging of the three-dimensional vectorial spin texture of the surface states of the $Bi_{1-x}Sb_x$ alloy series using state-of-the-art spin-resolved spectroscopy to quantitatively evaluate the TQNs. Based on both the measured spin polarization and spin chirality of the FSs, we observe that the bulk insulator not only belongs to the $\nu_{i=0} = 1$ class associated with time-reversal symmetry, but also carries a non-trivial mirror number associated with spatial symmetry. By monitoring the spin textures while tuning the system from a bulk insulating to a metallic state, we demonstrate that the surface states remain not only highly spin polarized but also topologically mirror class equivalent. Further, these topological spin states are found to be robust against the weak random-field perturbations induced via alloying, suggesting that a π Berry's phase on the surface survives in both bulk metallic and insulating phases.

In a non-polar 3D spin-orbit coupled insulator, the bulk states are spin degenerate due to a combination of space inversion symmetry $[E(\vec{k},\uparrow) = E(-\vec{k},\uparrow)]$ and time reversal symmetry $[E(\vec{k},\uparrow) = E(-\vec{k},\downarrow)]$. Since space inversion symmetry is broken at the surface, the spin degeneracy of surface bands can be lifted by the spin-orbit interaction. However, according to Kramers theorem, they must remain spin degenerate at four special time reversal invariant momenta (TRIM) in the 2D surface Brillouin zone (BZ), which for the (111) surface of $Bi_{1-x}Sb_x$ are located at $\bar{\Gamma}$ and three equivalent $\bar{M}$ points rotated by 60° from one another [Fig. 1(A)]. A total of four Z_2 topological numbers $\nu_0;(\nu_1\nu_2\nu_3)$ characterize a 3D time reversal invariant band structure [4, 6]. One in particular (ν_0) determines whether the FS formed by its 2D surface bands enclose the four TRIM an even or odd number of times, and consequently whether the material is in a weak ($\nu_0 = 0$) or strong Z_2 topological

insulator ($\nu_0 = 1$) phase respectively. To realize an odd number m of enclosures as shown in Fig. 1(A), such that electrons on the surface acquire a non-trivial Berry's phase of $m\pi$, the surface bands must be *spin polarized* and must cross the Fermi level (E_F) an odd number of times between two TRIM. If a spin-split pair emerging from one of the TRIM ($\bar{\Gamma}$) does not recombine at another TRIM ($\bar{\mathrm{M}}$) but rather "switches partners" this can be achieved. Therefore one must probe the "spin degrees of freedom" to investigate the nature of the topological quantum materials.

Spin-integrated ARPES intensity maps of the (111) surface states of insulating $Bi_{1-x}Sb_x$ taken at E_F [Figs 1(C)&(D)] show that a hexagonal FS encloses $\bar{\Gamma}$, while dumbbell shaped Fermi surfaces that are much weaker in intensity enclose $\bar{\mathrm{M}}$. By examining the surface band dispersion below E_F [Fig. 1(E)] it is clear that the central hexagonal FS is formed by a single band (Fermi crossing 1) whereas the dumbbell shaped FSs are formed by the merger of two bands (Fermi crossings 4 and 5) [19]. This band dispersion resembles the partner switching behavior characteristic of $\nu_0 = 1$ topological insulators, as the Kramers pair emerging from $\bar{\Gamma}$ (bands 1 and 2) do not recombine at $\bar{\mathrm{M}}$. To check this scenario we have carried out spin-resolved photoemission spectroscopy. Fig. 1(F) shows a spin-resolved momentum distribution curve (MDC) taken along the $\bar{\Gamma}$-$\bar{\mathrm{M}}$ direction at a binding energy E_B = -25 meV [Fig. 1(F)]. The data reveal a clear difference between the spin-up and spin-down intensities of bands 1, 2 and 3, and show that bands 1 and 2 have opposite spin whereas bands 2 and 3 have the same spin, all of which achieve high degree of polarization (detailed analysis discussed later in text). The former observation suggests and confirms that bands 1 and 2 form a time-reversal invariant Kramers pair, and the latter observation suggests that bands 2 and 3 are connected above E_F and form one band (which has implications for spatial symmetry). This is further confirmed by directly imaging the bands above E_F through raising the chemical potential [see supporting online material (SOM B)]. However due to a dramatic intrinsic weakening of signal intensity near crossings 4 and 5, and to the fact that the small energy and momentum splittings of bands 4 and 5 lie at the resolution limit of modern spin-resolved ARPES spectrometers, no conclusive spin information about these two bands can be drawn from the data [Figs 1(F)&(G)]. While our findings strongly suggest that the four TRIM on bulk insulating $Bi_{1-x}Sb_x$ (111) are enclosed by an odd number (7) of spin polarized surface FSs, it is important to find methods of manipulating this surface band structure so that its spin texture can be completely measured.

One way to manipulate the surface band structure of insulating $Bi_{1-x}Sb_x$ without altering ν_0 is to change the relative bismuth to antimony concentration. Figure 2(G) shows a schematic of the well studied evolution of the bulk band structure from $Bi_{0.91}Sb_{0.09}$ to pure Sb [20], with the insulator-to-metal transition occuring near $x = 0.2$ [20]. The $\nu_0 = 1$ character of $Bi_{0.91}Sb_{0.09}$ is derived from the relative energy ordering of the antisymmetric (L_a) and symmetric (L_s) states at the L point of the bulk 3D BZ [6, 20]. As the Sb concentration is increased, the insulating gap is closed by a hole like band at H rising above E_F and an electron like band at L sinking below E_F. Since this insulator-to-metal evolution of electronic structure preserves a finite direct inter-band gap at every point in $\vec{k}$-space as well as the relative energy ordering of the L_a and L_s states, the bulk valence and conduction bands continue to be connected only through surface states, and the connection scheme of these surface states between TRIM is expected to remain unchanged.

To investigate the connectivity of the surface bands of Sb(111) between TRIM, we first carried out spin-integrated ARPES measurements. Figure 2(A) shows a spin-integrated ARPES intensity map of Sb(111) from $\bar{\Gamma}$ to $\bar{M}$. By performing a systematic incident photon energy dependence study of such spectra, previously unavailable using He lamp sources [21], it is possible to identify two V-shaped surface states (SS) centered at $\bar{\Gamma}$, a bulk state (BS) located near k_x = -0.25 Å^{-1} (projection of bulk H point onto the surface BZ) and resonance states (RS) centered about $k_x = 0.25$ Å^{-1} and $\bar{M}$ that are hybrid states formed by surface and bulk states (SOM C). The overall experimental band dispersion is reproduced by tight binding calculations for a semi-infinite crystal of antimony [Fig. 2(B)]. As seen in both calculations and data, there is a pair of V-shaped surface bands, which resemble a spin-orbit split pair since they become degenerate at $\bar{\Gamma}$ (Kramers point), that lies completely within the projected gap of the bulk states so that their electron density is strongly localized at the surface. Conversely, the location of the measured resonance bands falls completely inside the calculated region of the projected bulk bands so that their wavefunction penetrates very deeply into the bulk, in turn causing their electron density to be less localized at the surface. The outer lying V-shaped SS band is seen to merge with the bulk valence band at H, while the inner lying V-shaped band merges with the bulk conduction band. Since no other states are observed in the projected bulk gap along $\bar{\Gamma}$-$\bar{M}$, this SS Kramers pair does not recombine at $\bar{M}$ and therefore exhibits a "partner switching" behavior.

To determine the topological class of the valence band of bulk metallic Sb, it is insufficient

to simply count the number of times the TRIM are enclosed by the FS, as is usually done for an insulator where no resonant states exist at E_F. This is because the density of states at E_F now also has a bulk contribution coming from the hole-like carriers at H and electron-like carriers at L, which couple strongly to the surface states near $k_x = 0.25$ Å^{-1} and $\bar{\text{M}}$ [Fig. 2(A)&(B)] leading to resonant behavior. The ARPES intensity map of the Sb(111) surface and resonance states at E_F [Fig. 2(C)] shows that there is one purely surface FS enclosing $\bar{\Gamma}$ that is formed by the inner V-shaped SS [Fig. 2(A)]. It also shows a tear drop shaped FS just outside $\bar{\Gamma}$ that is formed partly by the outer V-shaped SS and partly by a RS. Since this latter FS does not enclose any TRIM, it is topologically irrelevant. The resonance state FS enclosing $\bar{\text{M}}$ that lies within the projected areas of the bulk FS [Fig. 2(D)] can also be discounted because they can only contribute an even number of FS enclosures, which does not change the modulo 2 sum of TRIM enclosures (SOM D). With these considerations, it is clear that the surface FS of Sb(111) is consistent with a $\nu_0 = 1$ bulk band topology, due to a single FS enclosure of $\bar{\Gamma}$ by the Σ_2 band [Figs 2(C)&(B)]. And unlike the case in $Bi_{0.91}Sb_{0.09}$, the states near $\bar{\text{M}}$ are irrelevant.

To extract the *spin polarization vector* of each of the surface bands near $\bar{\Gamma}$, we performed high-resolution spin-resolved measurements using a Mott polarimeter. Spin-resolved MDC data sets along the -$\bar{\text{M}}$−$\bar{\Gamma}$−$\bar{\text{M}}$ cut at E_B = -30 meV [Fig. 3(B)] are shown for maximal intensity. A two-step fitting routine developed in [23] is used to fit the data. Spin detection is carried out using a Mott detector that is mounted so that at normal emission it is sensitive to a purely out-of-plane spin component (z') and a purely in-plane (y') spin component that is rotated by 45° from the sample $\bar{\Gamma}$ to -$\bar{\text{M}}$ direction [Fig. 3(A)]. Each of these two directions represents a normal to a scattering plane, defined by the electron incidence direction on a gold foil and two electron detectors mounted on either side that measure the left-right asymmetry $A_{y',z'} = [(I_L^{y',z'} - I_R^{y',z'})/(I_L^{y',z'} + I_R^{y',z'})]$ of electrons backscattered off the gold foil [24]. Figure 3(D) shows the spin polarization for both components given by $P_{y',z'} = (1/S_{eff}) \times A^{y',z'}$, where $S_{eff} = 0.085$ is the Sherman function. Following the vectorial spin analysis procedure described in [23], we take the 3D spin space vector of each band as fit parameters, assign a spin resolved spectra for each of the fitted peaks I^i shown in Fig. 3(C), and fit the calculated polarization spectrum to measurement. The spin resolved spectra for the y component derived from the polarization fit is shown in Fig. 3(E), given by $I_y^{\uparrow,\downarrow} = \sum_{i=1}^{4} I^i(1 \pm P_y^i)/6 + B/6$, where B is an unpolarized background and P_y^i is the

fitted y component of polarization. There is a clear difference in $I_y^{\uparrow}$ and $I_y^{\downarrow}$ at each of the four MDC peaks indicating that the surface state bands are spin polarized [Fig. 3(E)]. Each of the pairs $l2/l1$ and $r1/r2$ have opposite spin, consistent with the behavior of a spin split Kramers pair, and the spin polarization of these bands, which reach nearly 100%, are reversed on either side of $\bar{\Gamma}$ in accordance with the system being time reversal symmetric $[E(\vec{k},\uparrow) = E(-\vec{k},\downarrow)]$ [Fig. 3(F)]. The measured spin texture of the Sb(111) surface states (Fig. 3), together with the non-trivial connectivity of the surface bands between the surface TRIM (Fig. 2), uniquely determines its bulk TQN $\nu_0 = 1$. The singly degenerate spin down (Σ_2) band traverses the bulk inter-band gap in this semimetal. Therefore, the surface metal of bulk metallic antimony carries a non-trivial Berry's phase via the inner V-shaped band. These results show that Sb can be regarded as the parent metal of the Z_2 topological insulator in the sense that the topological Z_2 order originates from the parity set of the bulk Sb wavefunctions. Further evidence that the non-trivial surface FS topology of Sb continuously evolves from that of $Bi_{0.91}Sb_{0.09}$ comes from our ARPES spectra of 10% Bi substituted Sb [Figs 2(E)&(F)], which shows no effects on the surface state dispersion of Sb from the random alloy disorder potential.

Similar to the well known large spin-orbit coupling materials gold [25] and tungsten [26], the spin polarization of each band is largely in-plane [Figs 3(D)&(F)]. This implies that the electric field $\vec{E}$ at the terminated surface, which generates an effective magnetic field proportional to $(\vec{k} \times \vec{E})$, is predominantly out-of-plane. However unlike the case in gold, where the surface band dispersion consists of a pair of oppositely spin polarized parabolas that are offset in $\vec{k}$ by an amount proportional to the spin-orbit coupling strength [25], the pair of oppositely spin polarized surface bands of Sb(111) are highly non-parabolic. Each of these spin polarized surface bands is not reflection symmetric about its minimum, evidenced by the difference in Fermi velocity between bands $l1/r1$ (4.4 ± 0.1 eV·Å) and bands $l2/r2$ (2.2 ± 0.1 eV·Å) respectively, as found by fitting straight lines to their MDC peak positions. Due to the unusual dispersion of the two spin polarized surface bands, despite a modest offset between their minima of $\delta\vec{k} \sim 0.03$ Å^{-1} [Fig. 3(B)], and despite Sb having a relatively light atomic mass compared to gold, the $\vec{k}$ splitting between spin polarized surface bands near E_F is much greater in Sb (0.07 Å^{-1}) than in gold (0.026 Å^{-1} [25]). This property, together with a small density of spin degenerate bulk states at E_F due to its semimetallic nature makes Sb a promising candidate for high temperature spin current sources that are the central

component of many spintronic devices [27].

In addition to revealing the topological invariant related to the time-reversal symmetry, we show that our spin polarized measurement methods (Fig.1 and 3) probe an additional TQN related to the spatial symmetry of 3D topological insulators which is somewhat analogous to the spin-Chern number of 2D quantum spin Hall insulators. Bulk electronic states in the bulk mirror invariant ($k_y = 0$) plane can be classified in terms of an integer mirror Chern number n_M, which is zero in a trivial insulator ($\nu_0 = 0$), but can be any odd integer in a strong topological insulator ($\nu_0 = 1$) [12]. Analogous to how the *spin-Chern* number informs the number of 1D spin polarized edge states in 2D quantum spin Hall systems [18], the magnitude of n_M determines the number of spin polarized surface-edge states that traverse the bulk energy gap along the mirror invariant line connecting $\bar{\Gamma}$ to $\bar{\mathrm{M}}$ in the surface BZ [SOM F]. From figure 1, it is seen that a single surface state band, which switches partners at $\bar{\mathrm{M}}$, connects the bulk valence and conduction bands, so $|n_M| = 1$. The sign of n_M determines the mirror eigenvalue ($\pm i$) associated with the band that traverses the gap. This in turn is related to the direction of the spin polarization $\langle \vec{P} \rangle$ of this band at E_F, which is constrained by mirror symmetry to point along $\pm\hat{y}$. Since the central electron-like FS enclosing $\bar{\Gamma}$ intersects six mirror invariant points [Fig. 3(B)], the sign of n_M distinguishes two distinct chiralities for this spin polarized FS. Figures 1(E) and 3 show that for both $Bi_{0.91}Sb_{0.09}$ and Sb, the surface band that forms this electron pocket between $\bar{\Gamma}$ and $\bar{\mathrm{M}}$ has $\langle \vec{P} \rangle \propto -\hat{y}$. This demonstrates that both insulating $Bi_{1-x}Sb_x$ and metallic Sb belong to the same mirror Chern class, and further suggests that their bulk electron wavefunctions exhibit the anomalous value $n_M = -1$ predicted in [12], which is not realizable in free electron systems with full rotational symmetry.

Although a bulk insulator to metal transition from $Bi_{1-x}Sb_x$ to Sb is shown to alter the details of their surface state dispersion relations, our spin polarimetry measurements of their Fermi surface spin textures places both insulator and metal in the same ν_0 and mirror Chern topological class. The high degree of spin polarization observed in the bismuth rich alloy, where non spin conserving spin-orbit interactions are expected to be much more dominant than in antimony, is a measure of the robustness of these surface spin states against random disorder potentials. Quite generally, our results demonstrate that spin spectroscopy can be used as a novel tool for measuring quantum numbers associated with both time-reversal (ν_i) and spatial symmetries (n_M) in topological quantum metals or insulators that do not

exhibit any quantized spin or charge Hall transport. They also show that it provides a more direct probe of the existence of a Berry's phase compared to carrier density modulated Hall transport [29] measurements. This method can be applied to study other topological, spin Hall or Berry phase materials. The device-interfaces of these topological states with ordinary materials (superconductors or magnets) are expected to exhibit novel spin transport and exotic quasiparticle statistics, potentially opening a new avenue for the development of topological spintronics.

---

[1] F. Bloch, *Z. Phys.* **52**, 555 (1928).

[2] W. Kohn, *Phys. Rev.* **133**, A171 (1964).

[3] C. L. Kane, E. J. Mele, *Phys. Rev. Lett.* **95**, 146802 (2005).

[4] J. E. Moore, L. Balents, *Phys. Rev.* **B 75**, 121306(R) (2007).

[5] X. -L. Qi, T. Hughes, S. -C. Zhang, ⟨http://arxiv.org/abs/0802.3537⟩ (2008).

[6] L. Fu, C. L. Kane, *Phys. Rev.* **B 76**, 045302 (2007).

[7] K. v. Klitzing, G. Dorda, M. Pepper, *Phys. Rev. Lett.* **45**, 494 (1980).

[8] D. J. Thouless *et al.*, *Phys. Rev. Lett.* **49**, 405 (1982).

[9] B. I. Halperin, *Phys. Rev.* **B 25**, 2185 (1982).

[10] J. E. Avron, D. Osadchy, R. Seiler, *Phys. Today* **56**, 38 (2003).

[11] N. Nagaosa, *Science* **318**, 758 (2007).

[12] J. C. Y. Teo *et al.*, ⟨http://arxiv.org/abs/0804.2664⟩ (2008).

[13] L. Fu, C. L. Kane, *Phys. Rev. Lett.* **100**, 096407 (2008).

[14] X. -L. Qi *et al.*, *Nature Phys.* **4**, 273 (2008).

[15] Y. Ran, A. Vishwanath, D. -H. Lee, ⟨http://arxiv.org/abs/0801.0627⟩ (2008).

[16] J. E. Moore, Y. Ran, X. -G. Wen, ⟨http://arxiv.org/abs/0804.4527⟩ (2008).

[17] T. Grover, T. Senthil, *Phys. Rev. Lett.* **100**, 156804 (2008).

[18] M. König *et al.*, *Science* **318**, 766 (2007).

[19] D. Hsieh *et al.*, *Nature* **452**, 970 (2008).

[20] B. Lenoir *et al.*, Fifteenth International Conference on Thermoelectrics, 1-13 (1996).

[21] K. Sugawara *et al.*, *Phys. Rev. Lett.* **96**, 046411 (2006).

[22] Y. Liu, E. Allen, *Phys. Rev.* **B 52**, 1566 (1995).

[23] F. Meier *et al.*, *Phys. Rev.* **B 77**, 165431 (2008).

[24] M. Hoesch *et al.*, *J. Electron Spectrosc. Relat. Phenom.* **124**, 263 (2002).

[25] M. Hoesch *et al.*, *Phys. Rev.* **B 69**, 241401(R) (2004).

[26] M. Hochstrasser *et al.*, *Phys. Rev. Lett.* **89**, 216802 (2002).

[27] S. A. Wolf *et al.*, *Science* **294**, 1488 (2001)

[28] T. Hirahara *et al.*, *Phys. Rev.* **B76**, 153305 (2007).

[29] F. D. M. Haldane *Phys. Rev. Lett.* **93**, 206602 (2004).

[30] We thank J. C. Y Teo for providing the surface state band calculations of Sb, as well as B. A. Bernevig, A. V. Fedorov, L. Fu, D. Lu, F. D. M. Haldane and D. C. Tsui for discussions. This work is supported by the DOE Office of Basic Energy Science and materials synthesis is supported by the NSF MRSEC. C. L. K. was supported by NSF grant DMR-0605066.

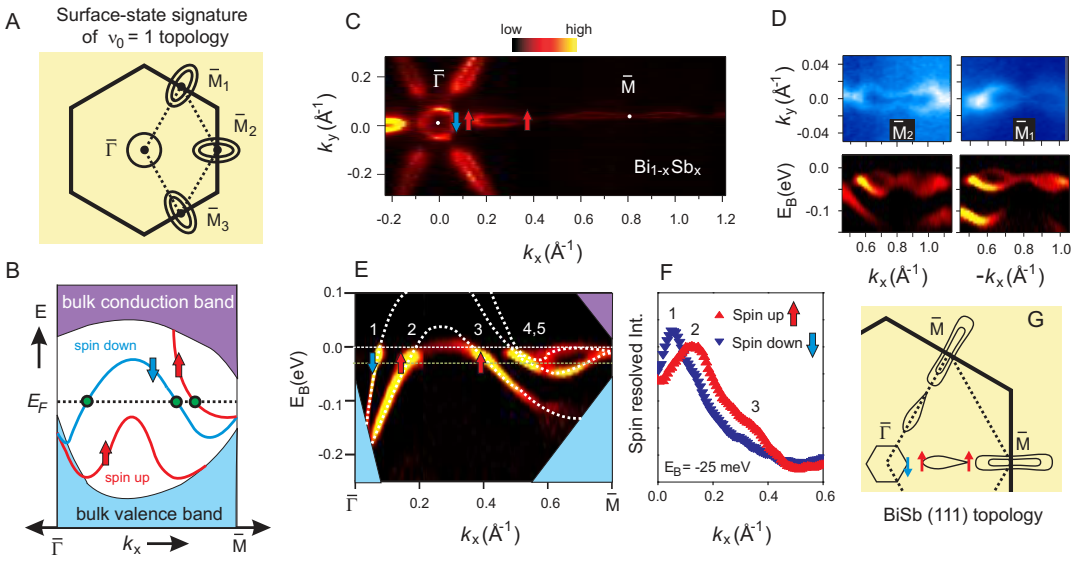

FIG. 1: **Theoretical spin spectrum of a $\nu_0 = 1$ topological insulator and spin-resolved ARPES spectroscopy results**. (**A**) Schematic of a Fermi surface (FS) formed by the spin-polarized surface states of a $\nu_0 = 1$ (strong) topological insulator. Each piece of the FS is necessarily singly degenerate in spin and altogether enclose the four Kramers degenerate points ($\bar{\Gamma}$, $\bar{M}_1$, $\bar{M}_2$, $\bar{M}_3$) an odd number of times. The points $\bar{M}_1$ and $\bar{M}_3$ are equivalent due to the three-fold rotational symmetry of the bulk crystal about the $\langle 111 \rangle$ axis, and are found to be equivalent to $\bar{M}_2$ based on our ARPES surface band dispersion maps. (**B**) The spin polarized (colored arrows) surface state dispersion between the two Kramers degenerate points at $\bar{\Gamma}$ and $\bar{M}$ that is required to realize the FS shown in (A). (**C**) Spin-integrated ARPES intensity map of the metallic surface states of bulk insulating $Bi_{0.91}Sb_{0.09}$ at E_F. Arrows point in the measured direction of the spin. (**D**) High resolution ARPES intensity map of the surface states at E_F that enclose the $\bar{M}_1$ and $\bar{M}_2$ points. Their corresponding band dispersion second derivative images are shown below. The left right asymmetry of the band dispersions are due to the slight offset of the alignment from the $\bar{\Gamma}$-$\bar{M}_1(\bar{M}_2)$ direction. (**E**) The surface band dispersion second derivative image along the $\bar{\Gamma}$-$\bar{M}$ direction showing five Fermi level crossings. The intensity of bands 4,5 is scaled up for clarity. Dashed white lines are guides to the eye. The shaded blue and purple regions corresponded to the schematic projection of the bulk valence and conduction bands respectively onto the (111) surface. (**F**) Spin resolved momentum distribution curves measured at E_B = -25 meV [green line in (E)] showing single spin degeneracy of bands at 1, 2 and 3. Spin up (down) corresponds to spin pointing along the +(-)$\hat{y}$ direction. Bands 4 and 5 cannot be resolved due to their extremely weak signal. (**G**) A schematic of the spin-polarized surface FS as measured by ARPES is shown in the right panel, and is consistent with a $\nu_0 = 1$ topological insulator phase.

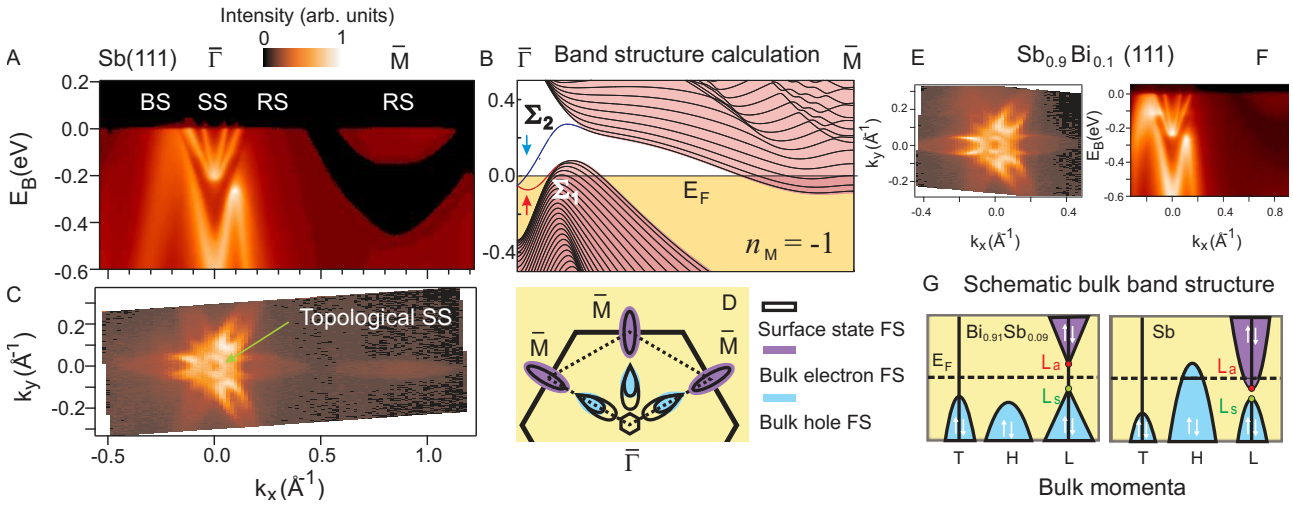

FIG. 2: **Non-trivial topological character of bulk metallic Sb revealed on the (111) surface states.** (**A**) Spin-integrated ARPES spectra of Sb(111) along the $\bar{\Gamma}$-$\bar{\mathrm{M}}$ direction taken with $h\nu$ = 22 eV photons. The surface states are denoted by SS, resonance states by RS and bulk states by BS. (**B**) Calculated surface state band structure of Sb(111) based on the methods developed in [12, 22]. The pink shaded regions denote the continuum bulk energy bands, and the lines show the discrete bands of a 100 layer slab. The red (blue) bands, denoted $\Sigma_{1(2)}$, are surface states with spin polarization $\langle \vec{P} \rangle \propto +(-)\hat{y}$. (**C**) ARPES intensity map at E_F in the k_x-k_y plane taken with $h\nu$ = 20 eV photons. The single-degenerate topological FS encircles the $\bar{\Gamma}$-point which is formed by the Σ_2 band. (**D**) Schematic picture of the surface FS of Sb(111) showing the pockets formed by the pure surface states (unfilled) and the surface resonances (blue and purple). The purely surface state Fermi contours enclose only one surface Kramers degenerate point located at $\bar{\Gamma}$, consistent with the $\nu_0 = 1$ topological classification of the bulk bands of Sb. (**E**) ARPES intensity map at E_F of 10% Bi substituted Sb(111) in the k_x-k_y plane taken using 20 eV photons, and its (**F**) dispersion intensity map along the $\bar{\Gamma}$-$\bar{\mathrm{M}}$ direction taken with $h\nu$ = 22 eV photons. Surface state features are robust against Bi alloy disorder (SOM E). (**G**) Schematic of the doubly spin degenerate bulk band structure of semiconducting $\mathrm{Bi}_{1-x}\mathrm{Sb}_x$ and Sb near the E_F. The topological Z_2 class of the bulk states is determined by the relative energy ordering of the L_a and L_s bands at the L point in the 3D bulk Brillouin zone, which does not change from $\mathrm{Bi}_{1-x}\mathrm{Sb}_x$ to Sb. The bulk T, L and H points project onto the $\bar{\Gamma}$, $\bar{\mathrm{M}}$ and $k_x \sim 0.25$ Å^{-1} points respectively on the (111) surface.

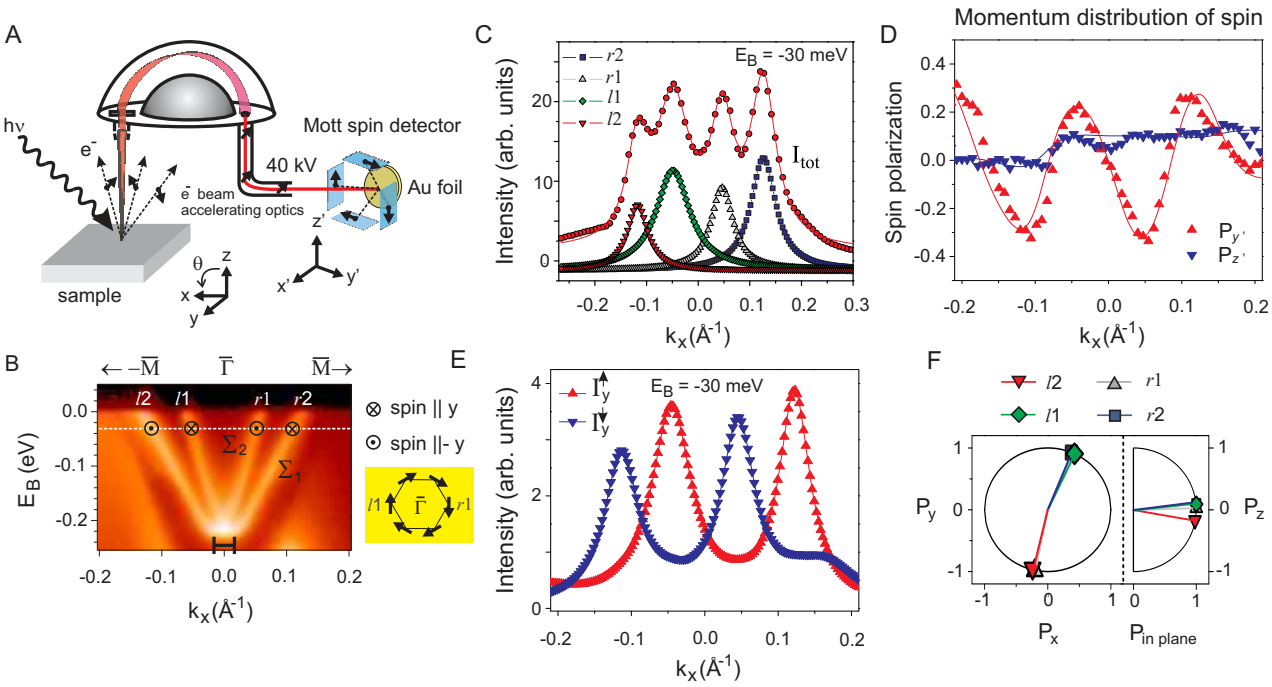

FIG. 3: **Spin-texture of topological surface-edge states**. (**A**) Experimental geometry of the spin-resolved ARPES study. At normal emission (θ=0°), the sensitive y'-axis of the Mott detector is rotated by 45° from the sample $\bar{\Gamma}$ to -$\bar{\mathrm{M}}$ ($\parallel$ -$\hat{x}$) direction, and the sensitive z'-axis of the Mott detector is parallel to the sample normal ($\parallel$ $\hat{z}$). (**B**) Spin-integrated ARPES spectra of Sb(111) along the -$\bar{\mathrm{M}}$−$\bar{\Gamma}$−$\bar{\mathrm{M}}$ direction taken using a photon energy $h\nu$ = 22 eV. The momentum splitting between the band minima is indicated by the black bar and is approximately 0.03 Å^{-1}. A schematic of the spin chirality of the central FS based on the spin-resolved ARPES results is shown on the right. (**C**) Momentum distribution curve of the spin integrated spectra at E_B = -30 meV (shown in (B) by white line) using a photon energy $h\nu$ = 20 eV, together with the Lorentzian peaks of the fit. (**D**) Measured spin polarization curves (symbols) for the detector y' and z' components together with the fitted lines using the two-step fitting routine. The measured polarization reaches a magnitude of around ±0.4, which is due to a non-polarized background and overlap of adjacent peaks with different spin polarization. The fitted parameters are in fact consistent with high degree (nearly 100%) of spin polarization. (**E**) Spin-resolved spectra for the sample y component based on the fitted spin polarization curve shown in (D). Up (down) triangles represent a spin direction along the +(-)$\hat{y}$ direction. (**F**) The in-plane and out-of-plane spin polarization components in the sample coordinate frame obtained from the spin polarization fit.